

Spiropyran-Based Photoisomerizable α -Amino Acid for Membrane-Active Peptide Modification

Andrii Hrebonkin,^[a, b] Sergii Afonin,^{*,[a]} Anna Nikitjuka,^[b, c] Oleksandr V. Borysov,^[b, c] Gundars Leitis,^[b, c] Oleg Babii,^[a] Serhii Koniev,^[b, d] Theo Lorig,^[a] Stephan L. Grage,^[a] Peter Nick,^[a] Anne S. Ulrich,^{*,[a]} Aigars Jirgensons,^[c] and Igor V. Komarov^{*,[b, d, e]}

Photoisomerizable peptides are promising drug candidates in photopharmacology. While azobenzene- and diarylethene-containing photoisomerizable peptides have already demonstrated their potential in this regard, reports on the use of spiropyrans to photoregulate bioactive peptides are still scarce. This work focuses on the design and synthesis of a spiropyran-derived amino acid, (S)-2-amino-3-(6'-methoxy-1',3',3'-trimethylspiro[2H-1-benzopyran-2,2'-indolin-6-yl])propanoic acid, which is suitable for the preparation of photoisomerizable peptides. The

utility of this amino acid is demonstrated by incorporating it into the backbone of BP100, a known membrane-active peptide, and by examining the photoregulation of the membrane perturbation by the spiropyran-containing peptides. The toxicity of the peptides (against the plant cell line BY-2), their bacteriotoxicity (*E. coli*), and actin–auxin oscillator modulation ability were shown to be significantly dependent on the photoisomeric state of the spiropyran unit.

Introduction

Peptides exhibit highly diverse biological activities and are promising therapeutics and theranostic tools.^[1] In particular, reversibly photoisomerizable (photoswitchable) bioactive peptides have attracted intense research attention for many decades.^[2] The photoregulation of peptides is achieved by incorporating light-responsive fragments, the so-called photoswitches, in their molecules, offering exciting prospects for drug development and *in vivo* studies of molecular processes using precisely focused optical stimuli as modulators.^[3] Hence, photo-

switch-modified bioactive peptides are promising drug candidates in a rapidly evolving medicinal chemistry area that is called “photopharmacology”^[4] and as research tools.

Most of the currently described photoswitchable peptides have been designed using azobenzene as the light-responsive unit.^[3b,c,g,i] In contrast, other known photoswitches, such as diarylethenes, stilbenes, hemithioindigos, fulgides, and spiropyrans, are underexplored in this structural context,^[3j] which is surprising given the vast knowledge accumulated on these photoswitches. For example, the photoinduced reversible transformation of spiropyrans (Figure 1) has been intensively studied since 1952.^[5] Spiropyrans belong to a unique type of photoswitches exhibiting diverse responsiveness to different stimuli.^[5f] However, spiropyran-modified bioactive compounds are still rare,^[6] even though conformational changes upon photoswitching were demonstrated decades ago for several spiropyran-modified proteins and polypeptides.^[3b,7] The influence of the environment on spiropyran-containing peptide photoisomerization equilibria and kinetics has been ingeniously used in analytical^[8] and imaging applications^[9] and for the development

[a] A. Hrebonkin, Dr. S. Afonin, Dr. O. Babii, T. Lorig, Dr. S. L. Grage, Prof. Dr. P. Nick, Prof. Dr. A. S. Ulrich
Karlsruhe Institute of Technology
POB 3640, 76021 Karlsruhe, Germany
E-mail: sergiy.afonin@kit.edu
anne.ulrich@kit.edu

[b] A. Hrebonkin, Dr. A. Nikitjuka, Dr. O. V. Borysov, Dr. G. Leitis, Dr. S. Koniev, Prof. Dr. I. V. Komarov
Enamine
Vul. Winstona Churchillia 78, 02094 Kyiv, Ukraine

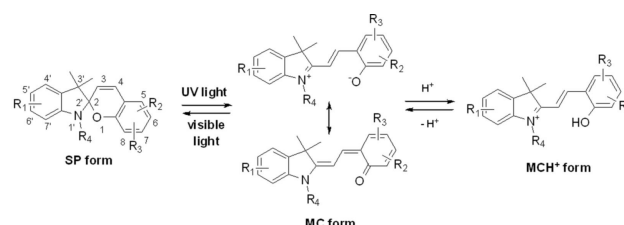
[c] Dr. A. Nikitjuka, Dr. O. V. Borysov, Dr. G. Leitis, Prof. Dr. A. Jirgensons
Latvian Institute of Organic Synthesis,
Aizkraukles iela 21, 1006 Riga, Latvia

[d] Dr. S. Koniev, Prof. Dr. I. V. Komarov
Taras Shevchenko National University of Kyiv
Vul. Volodymyrska 60, 01601 Kyiv, Ukraine

[e] Prof. Dr. I. V. Komarov
Lumobiotics
Auerstraße 2, 76227 Karlsruhe, Germany
E-mail: ik214@yahoo.com

Supporting information for this article is available on the WWW under <https://doi.org/10.1002/chem.202400066>

© 2024 The Authors. Chemistry - A European Journal published by Wiley-VCH GmbH. This is an open access article under the terms of the Creative Commons Attribution License, which permits use, distribution and reproduction in any medium, provided the original work is properly cited.



1a, R₁ = R₂ = R₃ = H, R₄ = Me; 1b, R₁ = R₂ = H, R₃ = 7-NEt₃, R₄ = Me; 1c, R₁ = R₂ = H, R₃ = 6-OMe, R₄ = Me; 1d, R₁ = R₂ = H, R₃ = 8-OMe, R₄ = Me; 1e, R₁ = H, R₂ + R₃ = 6,7-OCH₂O-, R₄ = Me; 1f, R₁ = R₂ = H, R₃ = 6-Ph, R₄ = Me; 1g, R₁ = R₂ = H, R₃ = 6-Br, R₄ = Me; 1h, R₁ = R₂ = H, R₃ = 6-Cl, R₄ = Me; 1i, R₁ = H, R₂ = 6-Br, R₃ = 8-Br, R₄ = Me; 1j, R₁ = H, R₂ = 6-Cl, R₃ = 8-Cl, R₄ = Me; 2a, R₁ = R₂ = R₃ = H, R₄ = (CH₂)₃NMe₃; 2b, R₁ = 5'-OMe, R₂ = R₃ = H, R₄ = (CH₂)₃NMe₃; 2c, R₁ = 5'-OMe, R₂ = R₃ = H, R₄ = (CH₂)₃SO₃H; 3, R₁ = 5'-OMe, R₂ = 6-CH₂CH(NH₂)CO₂H, R₃ = H, R₄ = Me;

Figure 1. Overview of the photoisomerization and acidochromism of spiropyrans, the model spiropyran-derived compounds studied in this work.

of photoresponsive hydrogels.^[10] However, the impact of spiropyran photoisomerization on the biological activity of peptides has been scarcely explored.^[11] One of the reasons for this *status quo* is the limited availability of photoswitch-containing building blocks suitable for the chemical synthesis of spiropyran-modified peptides. Almost none of the above-mentioned works used specifically designed spiropyran-based amino acids, which can be considered as the most appropriate building blocks.^[12]

A distinct advantage of spiropyran photoswitches is the dramatic change in structure and polarity induced by photoisomerization.^[5f] Spiropyran photoisomers (SP form, Figure 1) usually possess low polarity similar to that of hydrophobic proteinogenic amino acids, whereas merocyanine photoisomers (MC/MCH⁺ form, Figure 1) are highly polar/charged. Notably, both photoforms differ substantially in their structure and steric size. Therefore, we envisaged the development of a spiropyran-based α -amino acid whose major photoisomeric forms would mimic proteinogenic amino acids while differing in their steric size and polarity. The difference in the polarity of the SP and MC forms in the side chain should enable the modulation of the hydrophobic–hydrophilic balance (amphipathicity) of a peptide carrying such an amino acid. For many natural and synthetic membrane-active peptides, e.g., antimicrobial,^[13] fusogenic,^[14] and cell-penetrating^[15] peptides, this balance is important for their activity because it determines critical peptide–membrane interactions.^[16] We also hypothesized that photoisomerization of the spiropyran residue in an amphiphilic peptide could be an efficient tool to control its biological activity with light, at least concerning its membrane interactions, as was previously demonstrated for azobenzene-derivatized peptides.^[3b,c]

Herein, we describe the design, synthesis, and characterization of a spiropyran-based α -amino acid. We incorporated a novel amino acid into the membrane-active peptide BP100 and studied the effects of this modification on various BP100 interactions with lipid bilayers and living cells.

Results and Discussion

Design of spiropyran-derived α -amino acid

It is known that spiropyran photoswitches are not perfectly bistable.^[5f] Usually, only one photoform (either SP or MC) is stable in the absence of light, whereas the other form converts to the stable photoisomer in the dark. This process is known as thermally-induced “dark adaptation”. Under irradiation of the stable photoform, a photostationary state is usually established due to a competition between light- and thermally-induced isomerization. Considering these facts, we set the following criteria for the photophysical and chemical properties of the target amino acid toward the design of functional light-controllable peptides to be used in living organisms: (i) the thermally stable photoform of the modified peptides should be less biologically active than the thermally unstable photoform. In this case, the less active form of the peptides could be safely

applied to a living system, and its activity could then be switched “on” by light and turned “off” thermally in the absence of light, thereby minimizing side effects. (ii) The more active form of the peptides should be generated upon irradiation with visible light, preferably red light (~630–650 nm wavelength), because this light is less damaging to living organisms and penetrates deeper into the tissue of multicellular organisms than UV light. Combining both criteria, the thermally stable and less active spiropyran-based peptides should exist in their MC photoform and be capable of converting to the SP form under visible light irradiation. Spiropyran derivatives exhibiting such behavior were named “inverse (reverse, negative) photochromic systems”.^[17] (iii) As a third criterion, the MC-to-SP photoconversion should be as fast and complete as possible. (iv) In addition, the photoswitching molecular fragment must be sufficiently chemically stable, in particular, resistant to chemical degradation in aqueous media under physiological conditions and toward photodegradation upon irradiation.

Fulfilling simultaneously the above criteria is highly challenging. Although many known spiropyran photoswitches are thermally stable in the MC photoform in polar solvents, thus demonstrating the desired inverse photochromism [criterion (ii)],^[5f] the compounds reported as suitable for biological applications were poorly photoswitchable or photodegradable in most cases.^[18] In addition, most spiropyran fragments incorporated into polypeptides contain metabolically unstable nitro groups in the chromophore.^[3b,7a,b,10b] Nitro groups can cause toxicity issues *in vivo* and are avoided in drug candidates.^[19] Therefore, we first decided to synthesize model spiropyran-based compounds bearing substituents other than nitro groups at the spirocyclic core to determine the substitution pattern that favors inverse photochromism, efficient photoswitching, and sufficient chemical stability [criteria (ii)–(iv)].

Although the influence of substituents on the photoswitching properties of spiropyrans has been intensively investigated,^[20] the literature data are fragmentary and the measurements described in different publications were performed under different conditions. Thus, we compared the behavior of our model compounds under identical conditions in polar solvents.

In the first series of model compounds, we varied the R₂ and R₃ substituents in the benzopyran part of the core chromophore and synthesized compounds **1 a–j** (Figure 1) via the condensation reaction of various *o*-hydroxybenzaldehydes with 1,3,3-trimethyl-2-methylene-indoline (Fischer’s base) as a key synthetic step, which is the most widely used synthetic approach to spiropyrans.^[5d]

Since the compounds turned out to be insoluble in water, we selected methanol as another polar solvent to identify the substitution pattern that promotes inverse photochromism in a polar environment. The absorption spectra of compounds **1 a–j** in methanol revealed that the MC form was the prevailing stable photoisomer only in one case. Compound **1 b** bearing an electron-donating substituent NEt₂ in the benzopyran fragment exhibited a typical MC spectrum in the dark-adapted form (Figure 2; supplementary (SI) Figure S1).

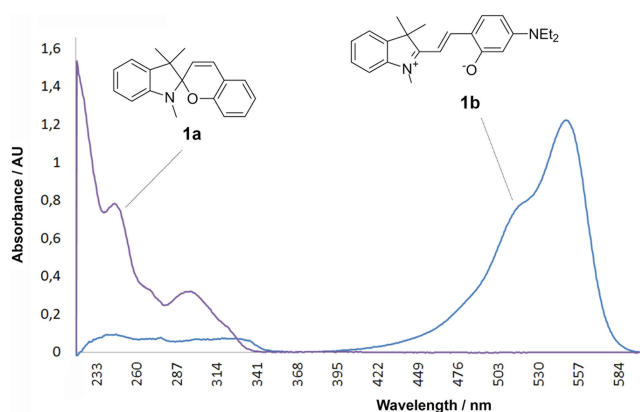


Figure 2. Representative absorption spectra of **1a** and **1b** recorded at a concentration of 10 μM in methanol in a 10 mm light path cuvette at ambient temperature after 30 min of dark adaptation.

MC stabilization by electron-donating substituents in the indoline fragment was previously reported for spiropyran photoswitches.^[20b,c] Therefore, we reconsidered the substitution pattern and installed an electron-donating substituent into the indoline fragment. We also attached a positively charged $(\text{CH}_2)_3^+\text{NMe}_3$ group to the nitrogen atom of the indoline fragment to increase the water solubility. Dark-adapted aqueous solutions of the resulting compound **2b** contained a much higher amount of the MC photoisomer than those of non-substituted **2a** (Table 1). Moreover, the MC form of **2b** could be converted almost completely into the SP form within minutes upon irradiation with visible light (420–550 nm).

Another known strategy for promoting the desired inverse photochromism is to introduce acidic groups at appropriate positions in the spiropyran chromophore.^[17a,21] Such groups can donate protons, which may further shift the equilibrium toward the fully protonated MCH^+ form in polar solvents (Figure 1).^[22] Thus, we synthesized model compound **2c** with an acidic group (SO_3H) to compare its behavior in water with that of **2a** and **2b**. As shown in Table 1 (see SI, Figure S2 for the ^1H NMR spectra), compound **2c** exhibited the most pronounced inverse photochromism. Interestingly, the MCH^+ content increased in

Table 1. Dark-adapted equilibria for compounds **2a–c**, measured via ^1H NMR in aqueous ~ 10 mM solutions at physiologically relevant pH values at 25 $^\circ\text{C}$.

Compound	R_1	X	MCH^+ content, %	
			pH 7.4	pH 5.5
2a	H	$^+\text{NMe}_3$	9	17
2b	OMe	$^+\text{NMe}_3$	11	63
2c	OMe	SO_3^-	59	ND ^[a]

[a] not determined

solutions at lower pH (compounds **2a** and **2b**), obviously due to protonation. Such proton-donating effects could stabilize the MC form in peptides bearing neighboring carboxylic or protonated amino groups in neutral and especially in acidic solutions.

Taken together, the model studies described above suggested that the inverse photochromism of the spiropyran moiety is maintained in peptides when the residue bears a 5'-OMe-substituted spiropyran core. The presence of abundant ionizable functional groups in peptides could further stabilize the MC form in aqueous solutions. Accordingly, we designed the target amino acid derivative bearing the fluorenylmethoxycarbonyl (=Fmoc) protecting group (N-Fmoc-**3**, Figure 1, Scheme 1).

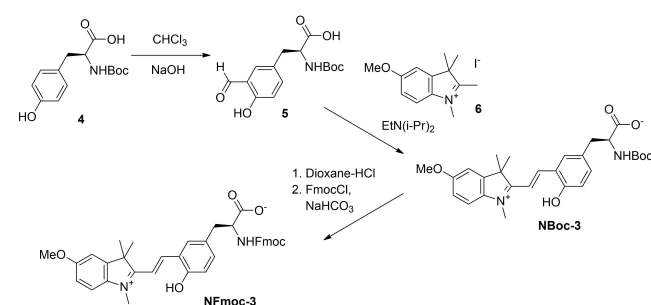
The synthesis of N-Fmoc-**3** was performed starting from N-Boc-protected natural L-tyrosine **4** (Scheme 1).

Design and synthesis of the photoswitchable analogs of BP100

The next step was to incorporate **3** into a peptide sequence using solid phase peptide synthesis (SPPS), Fmoc chemistry. We selected the representative membrane-active α -helical peptide BP100 (KKLFKILKYL-NH₂),^[23] whose conformational and functional features are well known. To satisfy criteria (i) and (ii), a careful choice of the position of **3** in place of a natural amino acid residue in the BP-100 sequence was required.

The sequence of BP100 was designed as a chimera from two natural antimicrobial peptides, i.e., cecropin A (from the moth *Hyalophora cecropia*) and melittin (the main component of the *Apis mellifera* venom), representing a peptide that was specifically developed to treat plant infections.^[23] This peptide is amphiphilic because it folds into an α -helix and can interact with various cell membranes.^[24] We aimed to synthesize a BP100 analog that was less active in the dark due to a perturbed amphiphilic profile but whose membrane interactions could be boosted by switching the spiropyran fragment under visible light.

We reasoned that the polar MC photoform (dark-adapted) should perturb the amphiphilic character of the peptide when situated on the hydrophobic face of the BP100 α -helix. Therefore, we considered BP100 analogs in which **3** substituted the natural hydrophobic Ile7 or Phe4 residues. We may anticipate



Scheme 1. Synthesis of the target α -amino acid **3** in N-Fmoc-protected form.

that the amphiphilicity of BP100 can be restored upon MC-to-SP photoswitching because the SP photoisomer possesses low polarity. Figure 3 illustrates the peptide design and sequences of the BP100 analogs. We synthesized two spiropyran-containing analogs: monosubstituted BP100-7MC [KKLFKK(3)LKYL-NH₂] and disubstituted BP100-4,7MC [KKL(3)KK(3)LKYL-NH₂]. N-Fmoc-3 was fully compatible with standard SPPS protocols; the spiropyran-modified peptides were obtained in moderate yields with high purity (>95%) after HPLC purification (SI, Figure S3).

Characterization of spiropyran-containing peptides

Both BP100-7MC and BP100-4,7MC were soluble in phosphate buffer (PB) at pH values spanning the entire physiological range (5–8).^[25] As predicted in the design of **3** based on the data for our model compounds, the absorption spectra of the peptides in these solutions were characteristic of the MC photoforms (SI, Figure S4).^[26] The absorption of the MC forms was pH dependent, as illustrated in Figure 4A for BP100-7MC. Upon increasing pH, an increase in absorbance at $\lambda_{\text{max}}=550$ nm and a gradual disappearance of the band at $\lambda_{\text{max}}=425$ nm were observed. This pH dependence is a known phenomenon for merocyanines^[27] and reflects the equilibrium between protonated MCH⁺ and nonprotonated MC forms.

Next, we studied the light-induced photoisomerization and thermally-induced dark adaptation of the two peptides at different pH values. Irradiation of acidic, neutral, and alkaline solutions with blue light ($\lambda=460$ nm, power density 1000 mW/cm²) resulted in a fast (~10 s) decoloration. The UV spectra of the decolorized solutions corresponded to the SP forms of the photoswitch chromophore,^[28] demonstrating the required inverse photochromism of both peptides.

A quantitative comparison of the irradiated spectra with the spectra of pure MC forms revealed that the MC-to-SP photoisomerization of peptides proceeded almost completely. Notably, a fast MC-to-SP photoisomerization of the two peptides was observed at pH 7 and 8 even upon irradiation with a redshifted light of 570 nm wavelength (yellow), which is important for *in vivo* applications.

The SP-to-MC adaptation of peptides in the dark proceeded with complete restoration of the initial MC photoforms within minutes in most cases, as illustrated in Figure 4B, except for the solutions of BP100-4,7MC at pH 7.0 and 8.0. Under these conditions, the dark-adapted spectra of BP100-4,7MC were not identical to the initial spectra (pure MC forms), indicating that certain amount of SP form remained in equilibrium with the MC form even after prolonged relaxation.

The MC forms of the peptides exhibited weak fluorescence with maxima at ~550 nm upon excitation at 440 nm. The fluorescence of the spiropyran side chain can be used as a sensor to probe the local environment in living cells.^[9,11] The fluorescence intensity was pH dependent, reaching the highest value at the lowest pH measured (5.0). In the presence of excess sodium dodecylsulfate (SDS) micelles, the fluorescence intensity increased sharply and almost lost its pH dependence (Figure 4C, 4D and Supplementary Figure S5).

Our peptides underwent no remarkable photodegradation; the degradation of BP100-7MC was less than 7% after 15 photoswitching cycles in pH 6.0 PB (Figure S4).

Structure of photoswitchable BP100 in membrane-mimicking environments

The conformational behavior of the peptides was studied for the MC form using circular dichroism (CD) spectropolarimetry,

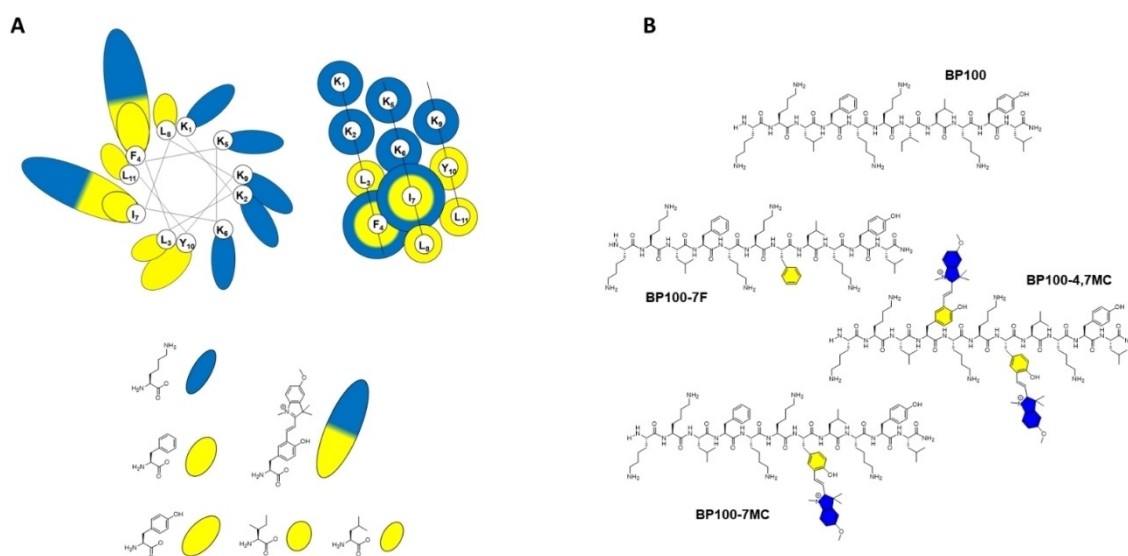


Figure 3. Peptides used in this study. (A) Amphiphilicity of the α -helically folded BP100. Helical wheel (top left) and helical mesh (top right) representations of amino acids in one-letter code. The polar amino acids are displayed in blue, the nonpolar ones in yellow, and the photoswitchable spiropyran residue in yellow/blue. (B) Structures and nomenclature of the studied peptides. The residue **3** is shown in the MC photoform.

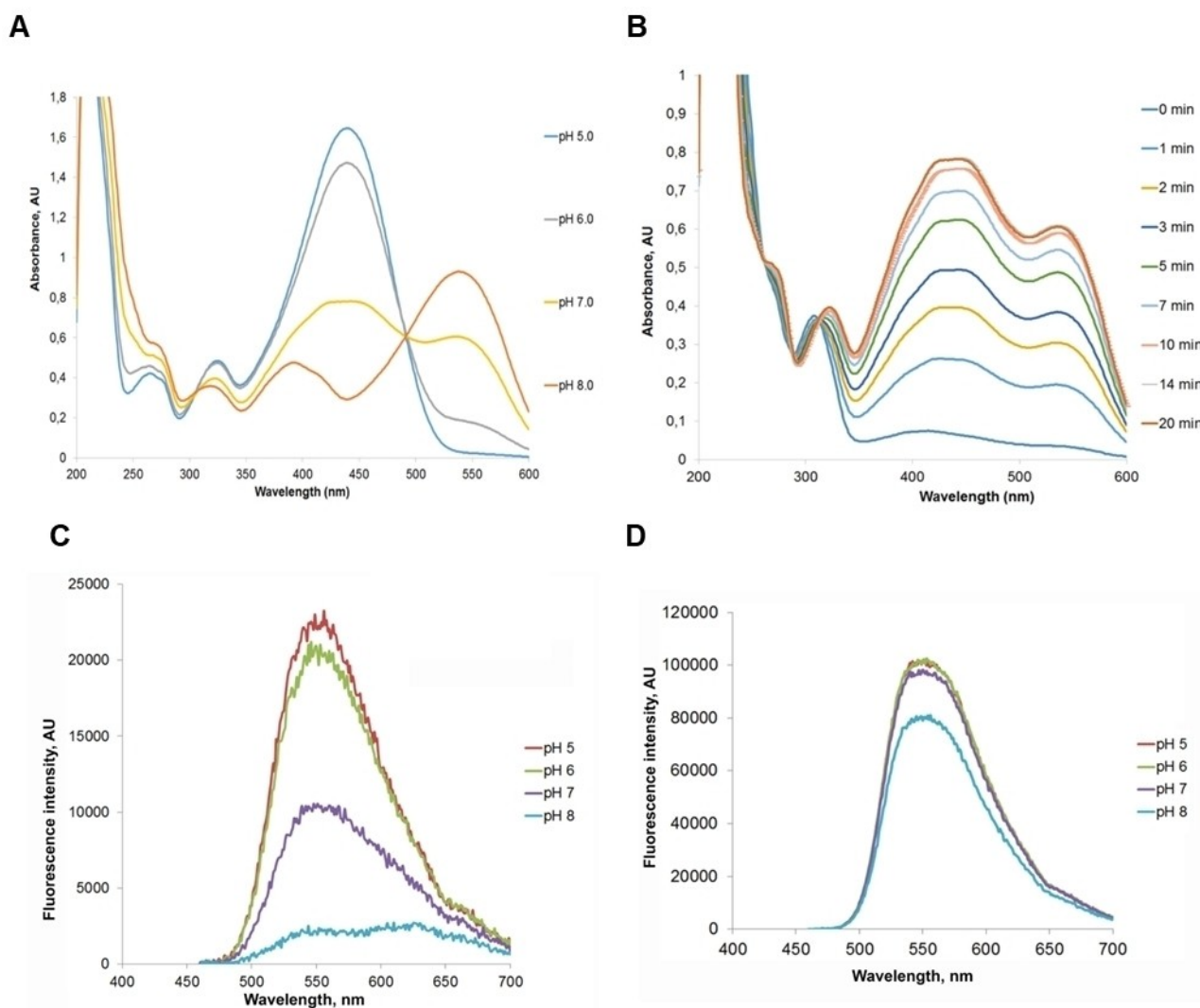


Figure 4. Spectroscopic characterization of photoswitchable peptides. (A) Absorption spectra of aqueous BP100-7MC solutions at different pH values (measured in 10 mM buffers, 100 mM NaCl, r. t.) and a peptide concentration of 70.4 μM . (B) Kinetics of the dark adaptation of the spiropyran moiety of BP100-7MC in PB (pH 7). Fluorescence spectra of BP100-7MC recorded (C) at different pH values and (D) in the presence of SDS micelles. See SI for the specific conditions.

and the results were compared with those of the nonphotoswitchable original peptide BP100 and the phenylalanine mutant BP100-7F. CD spectra were collected in aqueous buffers and in media mimicking cell membranes, i. e., 50% 2,2,2-trifluoroethanol (TFE) in PB, micellar solutions of anionic sodium dodecyl sulfate (SDS) and zwitterionic dodecylphosphorylcholine (DPC), and large unilamellar vesicles (LUV, *ca.* 100 nm diameter) prepared from 1,2-dimyristoyl-*sn*-glycero-3-phosphocholine (DMPC) and 1,2-dimyristoyl-*sn*-glycero-3-(phospho-*rac*-(1-glycerol)) (DMPG) (1:1 molar ratio). Representative CD spectra are shown in Figure 5.

All peptides were largely unstructured in aqueous environment irrespective of pH. In the hydrophobic helix-promoting PB/TFE mixture, the peptides showed characteristic helix CD signals, with the intensity and degree of helicity decreasing in the order: BP100 > BP100-7F > BP100-7MC > BP100-4,7MC. This behavior strongly suggests a considerable helix-perturbing

potential of the spiropyran residue in the MC form, as anticipated. When reconstituted in both types of SDS and DPC micelles, the spectra of the peptides demonstrated the same trend, but also revealed additional features. Thus, BP100 and BP100-7F displayed the typical α -helical CD spectra with characteristic negative bands at 208 and 222 nm of similar intensity, whereas the 3-derived peptides showed a different $n \rightarrow \pi^*$ transition signal at around 230 nm, containing a positive ellipticity feature around 220 nm for BP100-4,7MC. The spectrum of BP100-7MC reflects a reduced helicity, while the positive signal at 220 nm in the spectrum of BP100-4,7MC suggests the presence of a kinked or partially unfolded structure probably associated with the residue of 3 at the fourth position. Finally, in the presence of LUVs, only BP100 was helical and well folded.

In a separate set of experiments, we photoisomerized the spiropyran-modified peptides *in situ* and compared the CD

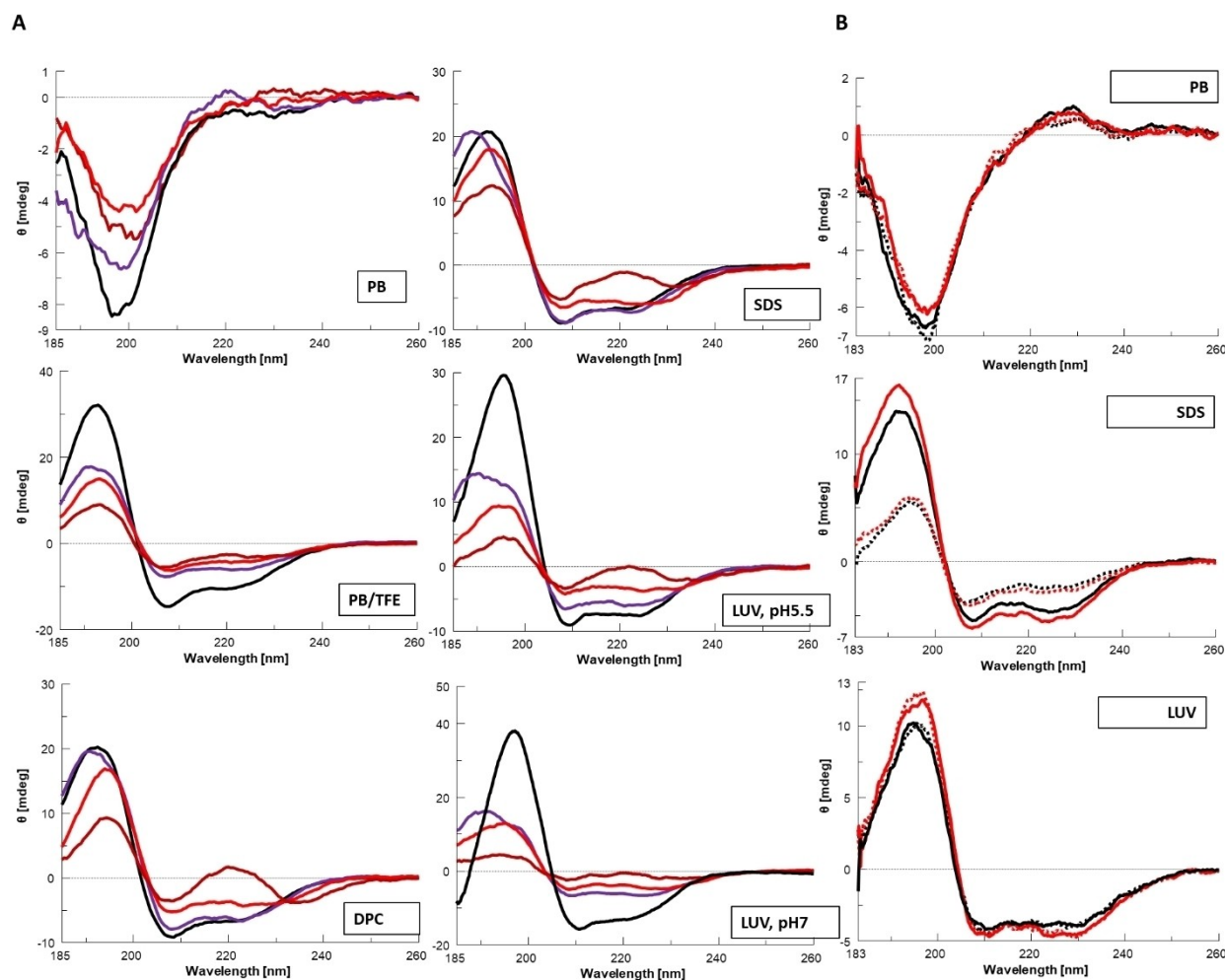


Figure 5. Structural studies of BP100 analogs in membrane-mimicking environments. (A) CD spectra of the peptides in 10 mM PB, PB/TFE, isotropic micelles (DPC and SDS, 7 mM) at pH 5.5, 140 mM NaF, 25 °C: BP100, black; BP100-7F, violet; BP100-7MC, light red; BP100-4,7MC, dark red. Peptides reconstituted in DMPC/DMPG LUVs (peptide/lipid = 1/20, mol/mol) are shown at pH 5.5 and 7.0. The peptide concentration in all samples was 70 or 100 μ M for LUVs. (B) Photoswitching (MC-to-SP photoisomerization) of the spiropyran-containing BP100 analogs in PB (top), in the presence of membrane mimics (5 mM SDS solution, middle), and in lipid bilayers (DMPC/DMPG LUVs, bottom). BP100-7MC, red; BP100-4,7MC, black; MC photoform of the side chains, dotted lines; SP photoform, solid lines.

spectra in PB, SDS, and LUV environments at pH 7.0. As seen in Figure 5B, substantial photoinduced structural changes occurred in both spiropyran-modified peptides in SDS and, to a lesser extent, in DPC (data not shown). We note, that the obvious differences of the MC spectra in SDS may be attributed to the below cmc conditions of the latter experiment (cmc = 7–8 mM).

Interactions between photoswitchable BP100 analogs and lipid membranes

Next, we compared the peptides containing **3** with BP100 and BP100-7F in lipid bilayers mechanically oriented between thin glass slides (see the samples preparation in the Experimental Section) using solid-state NMR spectroscopy (ssNMR). First, we characterized peptide-induced bilayer perturbations via ^2H ssNMR in zwitterionic DMPC- d_{54} and anionic DMPG- d_{54} .

Changes in the quadrupolar splitting of perdeuterated glycerophospholipids in the fluid lamellar phase in the presence of BP100 compared with pure bilayers are indicative of a strong bilayer thinning.^[29] We observed thinning with all our peptides in the fluid DMPG- d_{54} and DMPC- d_{54} bilayers ($T > 23$ °C) (Figure 6A). In contrast, membrane thickening due to interaction with the peptides was observed in gel bilayers ($T < 23$ °C) in both DMPC- d_{54} and DMPG- d_{54} .

We further performed ^2H ssNMR measurements of the same samples upon *in situ* MC-to-SP photoswitching (Figure 6B). Irradiation of the samples containing BP100-7MC and BP100-4,7MC caused decoloration and changes in the ^2H ssNMR spectra. Above the phase-transition temperature, the splittings increased by approximately 3 kHz during irradiation, indicating that switching from the MC to the SP forms resulted in lesser bilayer thinning.

Using ^{31}P ssNMR in 1,2-di-(9Z-octadecenoyl)-*sn*-glycero-3-phosphoethanolamine (DOPE) bilayers, we evaluated the

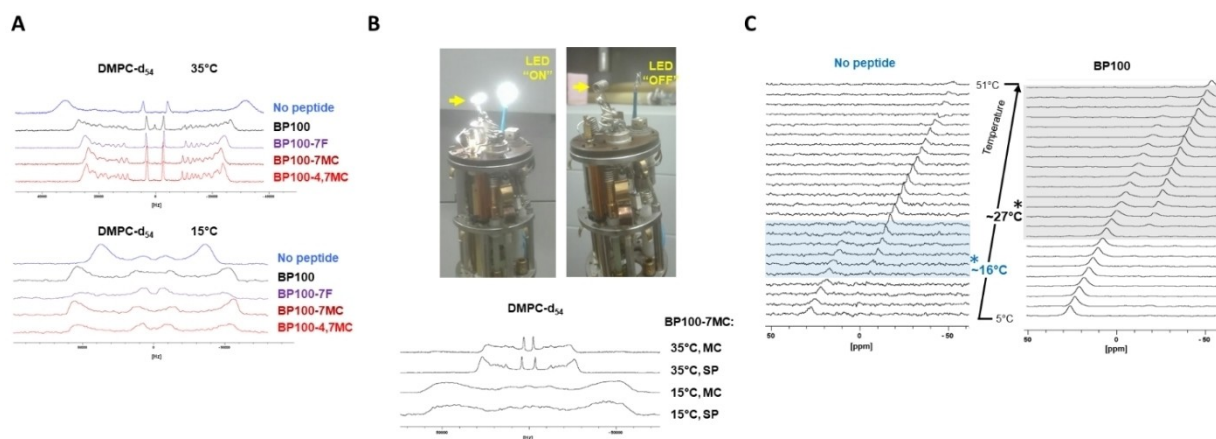


Figure 6. Solid-state NMR (ssNMR) studies of peptide/lipid interactions. (A) Representative ^2H ssNMR spectra of BP100 analogs in proteobilayers of DMPC- d_{54} . The spectra were measured above (35 °C, top stacks) and below (15 °C, bottom stacks) the main thermotropic phase transition (T_m , ca. 23 °C). Fully hydrated proteobilayers with peptide/lipid = 1/10, mol/mol; spiropyran-modified peptides are in the dark-adapted form (MC). (B) Photoswitching (MC-to-SP photoisomerization) of the spiropyran-containing BP100 analogs. Top: installment of an LED into a static ssNMR probe. The arrow points to the sample-containing coil. Bottom: representative spectra in darkness ("MC") compared with the spectra under continuous LED illumination ("SP"). The traces above (35 °C) and below (15 °C) T_m were measured for B100-7MC in DMPC- d_{54} . (C) Representative ^{31}P ssNMR spectra of supported DOPE membranes undergoing thermotropic L_α -to- H_{II} phase transition. Pure lipid (left column) compared with the BP100/lipid ratio of 1/100, mol/mol, mixture (right column). T_{L-H} (maximum) of the transition is indicated with an asterisk. The temperature range in which both phases coexist is highlighted with a background color.

impact of BP100 and its analogs on the bilayer curvature. Since the lipid headgroup-associated surface of phospholipid assemblies is negatively curved in the inverted hexagonal phase state (H_{II} phase, inverted cylindrical micelles), and the lamellar phase state (L_α phase) can be assumed to have a close to zero curvature, the transition between two phases can be associated with the induction of a positive or negative curvature by membrane-active compounds.^[30] Temperature-dependent ^{31}P ssNMR spectra were collected using samples of peptide/DOPE bilayers aligned on the glass slides (as above). As shown in Figure 6C, BP100 and its analogs increased (ca. 11 °C) and broadened the DOPE phase transition, unambiguously demonstrating a positive curvature induction even at low peptide concentrations (peptide/lipid = 1/100 mol/mol). The phase-transition temperature further increased by an additional 3 °C–6 °C upon *in situ* irradiation of the BP100 analogs inducing the SP forms.

Bioactivity of photoswitchable BP100 analogs

To determine whether the differential behavior of the 3-derived BP-100 photoforms in lipid membranes described in the previous section manifests itself in living cells, we checked the toxicity of the novel peptides against a tobacco cell line, *Nicotiana tabacum* L. cv. Bright Yellow No. 2 (BY-2)^[31] because BP100 was developed to treat plant pathogens.

BY-2 cell death induced by BP100 and its analogs at different concentrations was assessed via microscopy (Figure 7A). We qualitatively demonstrated *in situ* cytotoxicity photoswitching for samples containing 32 $\mu\text{g}/\text{mL}$ of the spiropyran-modified peptides after incubation with the cells for 2 h. A photoinduced cytotoxicity enhancement was observed for both spiropyran-containing peptides (Figure 7B). A moder-

ate increase in cell toxicity was induced by irradiating the cultures containing the peptides bearing 3, causing the MC-to-SP photoisomerization.

We were surprised to observe overall high cytotoxicities against eukaryotic (plant) cells because BP100 is considered an antibacterial peptide with a relatively high therapeutic index.^[32] The standard culturing pH for plant cells is somewhat acidic (pH 5.8), whereas antibacterial and hemolytic activities are generally measured at neutral values. Considering that the pH lowering may affect the MCH^+/MC equilibrium (see Table 1 and Figure 1 and 4), resulting in a more pronounced difference in amphiphilicity for our photoswitchable BP100 analogs (SP photoforms being apolar, MC polar, and MCH^+ charged), we studied the pH dependence of the antibacterial cytotoxicity of our peptides. As can be seen in Figure 7C, the SP photoforms of both 3-substituted peptides were bacteriotoxic at pH 5 (16 μM concentration). In contrast, the photoisomerized peptides with destroyed amphiphilicity exerted virtually no effect on the growth of overnight cultures at this concentration, at any pH. The pH dependence of the BP100 bioactivity is intriguing but was not the focus of our study. We were delighted to find conditions affording dramatic differences in the amphiphilicity-dependent bioactivities.

Finally, the photoswitchable BP100 analogs were evaluated for their ability to interfere with the actin–auxin oscillator of plant cells, for which BP100 is active when applied at nontoxic concentrations and with short exposure times.^[33] In these experiments, after the addition of the peptides photoisomerized to the SP forms (continuously illuminated with a white-light LED), the cells were immediately transferred to the microscopy stage to ensure that the photoconversion of the SP-to-MC photoforms occurred in real time.

This observation revealed dark adaptation-associated changes in actin remodeling (Figure 8). Remarkably, the SP

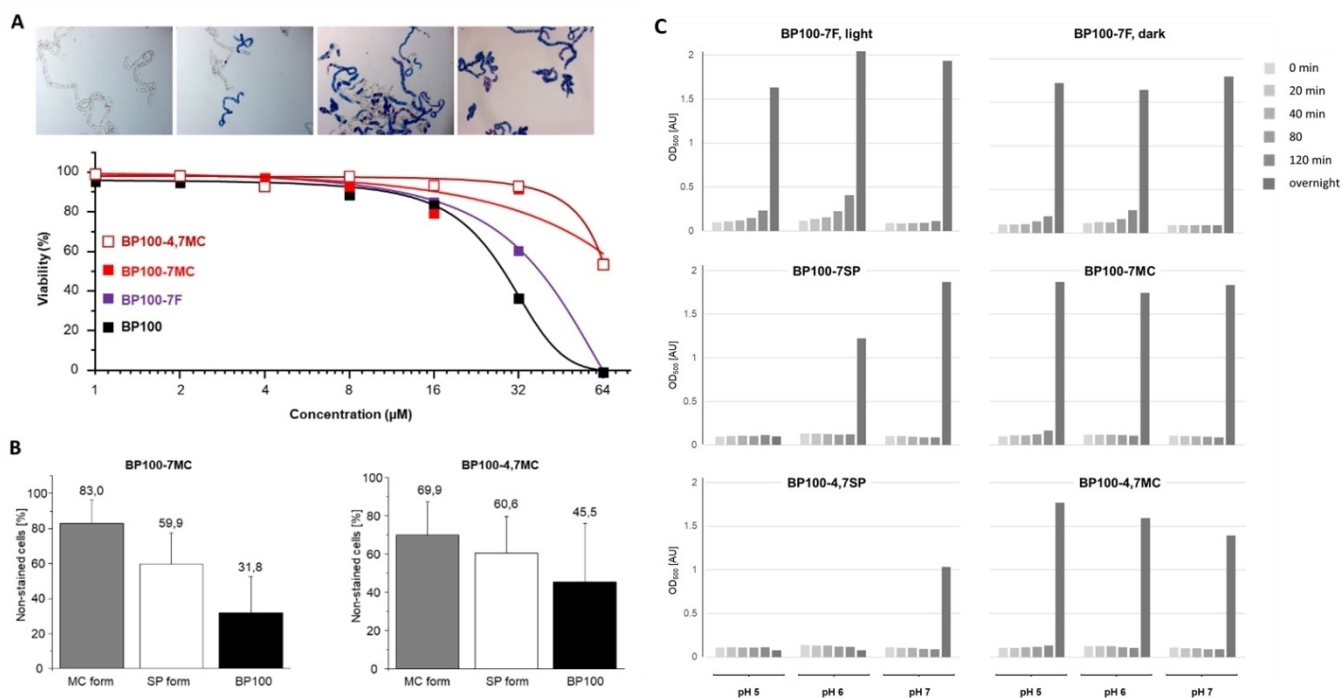


Figure 7. Cytotoxicity of the spiropyran-modified BP100 analogs. (A) Photographs of the cytotoxicity assessment of BP100 against BY-2 cells (left to right): 100%, 66%, 33%, and 0% nonstained (alive) cells. Results of cell counting (% alive) for the four peptides at different concentrations after 24 h coincubation. Photoswitchable peptides in the MC photostate. (B) Comparison of the cytotoxicity of BP100 and its analogs against BY-2 cells (peptide concentration, 32 μ M; incubation with cells, 2 h). (C) pH dependence of the antibacterial activity (*E. coli*) of BP100 analogs. Nonphotoswitchable, BP100-7F, and spiropyran-modified BP100 analogs were added to bacterial suspensions at 16 μ M and incubated under continuous white LED light illumination (left column, indicated as “light” or “SP”) or in darkness (right column, indicated as “dark” or “MC”).

photoisomers of both photoswitchable peptides caused filament contraction at almost the same level as the wild-type peptide. After approximately 90 s, when most of the spiropyran residues should have been converted to the MC photostates, the actin dynamics restored to levels compatible with the control (nontreated) cells (Figure 8G). Overall, this result suggests that for the BP100-induced actin–auxin oscillator modulation, the amphiphilicity of the peptide is important, and that a photoisomeric state of the residue 3 can modify the biological activity of 3-derived membrane-active peptides.

Conclusions

In summary, we demonstrated the utility of a spiropyran photoswitch for modulating the structure and function of a membrane-active peptide using the known peptide BP100 as a representative example. Amino acid 3 bearing a spiropyran core in its side chain was designed to fulfill strict criteria for the practical application of the corresponding peptides in living systems. Photoswitchable analogs of BP100 in SP and MC photostates were found to be differentially active in the induction of membrane thinning and in membrane curvature modulation. Furthermore, their helicity substantially differed in detergent solutions, and their cytotoxicity correlated with the degree of structuring, being lower in the MC photostates where amphiphilicity was destroyed. In the SP photostates, BP100

analog demonstrated a degree of actin dynamics modulation similar to that of the wild-type peptide in live plant cells. In contrast, the MC isomers did not interfere with cell cytoskeleton dynamics. This work has laid out the fundamental design principles for spiropyran-derived photoswitchable amino acids, paving the way for future applications of spiropyran-modified peptides in photopharmacology and beyond.

Experimental Section

Additional supporting data and analytical spectra are shown in the Supplementary Information.

General: All chemicals and solvents used for the syntheses were purchased from commercial vendors (Merck, ABCR, Carl Roth, Bachem, Biosolve, Enamine) and were not purified further, if not indicated. Synthetic reactions for the model compounds and the amino acid 3 were controlled by analytical thin-layer chromatography (TLC). TLC plates coated with silica gel 60 F254 (Merck) were used.

Flash chromatography was performed on Biotage FLC using C18 silica gel. Analytical ^1H and ^{13}C NMR spectra were recorded on 300, 400 or 500 MHz Bruker spectrometers with chemical shift values (δ , ppm) using the residual solvent signal as an internal reference. Exact molecular masses (HRMS) were determined with an LTQORBITRAP XL THERMO instrument. Analysis by liquid chromatography with mass spectrometry detection (LCMS) was performed employing an Agilent 1200 series LC instrument coupled with a Waters mass spectrometry system, equipped with ESCi multi-mode ioniza-

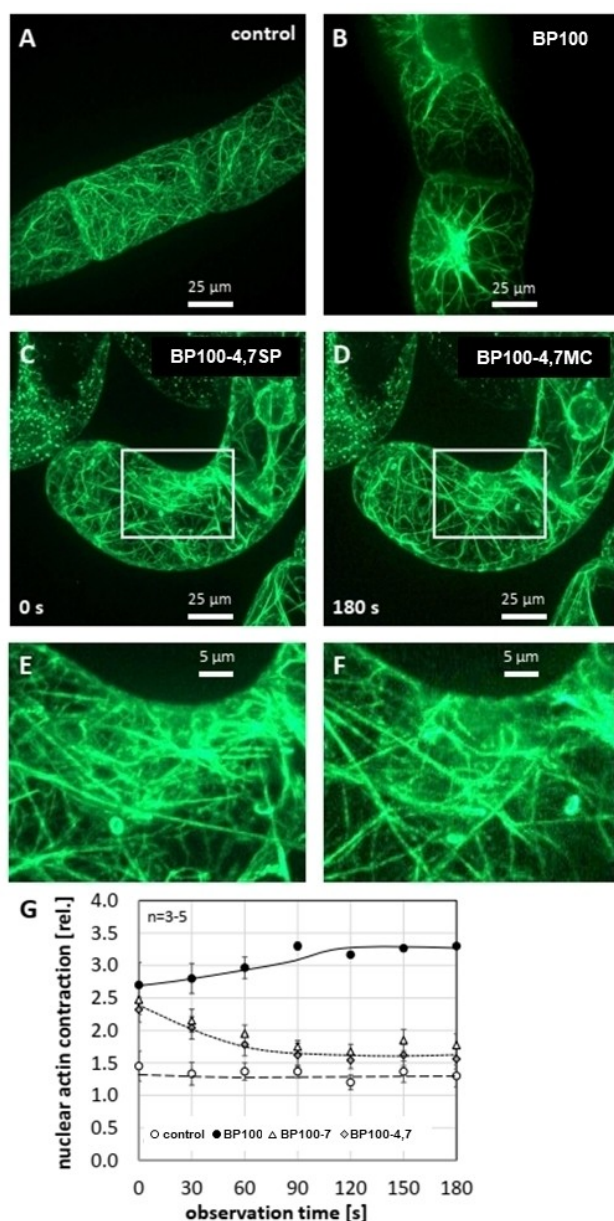


Figure 8. Response of plant actin filaments to BP100 and its photoswitchable analogs. Representative tobacco BY-2 cells expressing the actin-binding domain 2 of fimbrin 1 from *Arabidopsis thaliana* in fusion with GFP were imaged via spinning-disc confocal microscopy without treatment (control, A) and in the presence of 5 μ M of BP100 (BP100, B) and BP100-4,7, respectively, during SP-to-MC isomerization (BP100-4,7SP/BP100-4,7MC, C–F). (C) Representative first frame (0 s) of a cell treated with BP100-4,7 in the SP photostate and (D) image of the same cell 180 s later. To evaluate the changes in nuclear actin contraction, the regions within the white rectangles in C and D were magnified (E and F, respectively). (G) Time-dependent changes in nuclear actin contraction in the presence of different peptides, quantified from the time-lapse series according to³⁴. Data represent mean and standard error (three to five individual cells were examined).

tion source and a Micromass ZQ mass detector. High-performance liquid chromatography (HPLC) of peptides was done using a Jasco system with a diode-array detector. Purification of the peptides employed a 22 \times 250 mm C18 Vydac (300 \AA , 10 μ m) column. Analytical HPLC employed a 4.6 \times 250 mm C18 Vydac (300 \AA , 5 μ m) column. Eluent A: 90% 5 mM HCl, 10% acetonitrile (MeCN); eluent B: 90% MeCN, 10% 5 mM HCl. Purified peptides were stored as

lyophilized powders. Mass spectra of the peptides were recorded on a Bruker Autoflex III instrument using matrix-assisted laser-induced desorption/ionization (MALDI-MS) with TOF (time of flight) detection.

Synthesis of model compounds: Known compounds **1** and **2** were synthesized following the procedures described in the literature.^[27,35,36] Analytical data correspond to the literature reports.

1',3',3'-trimethyl-1',3'-dihydrospiro[chromene-2,2'-indole] (**1 a**): ¹H NMR (400 MHz, DMSO) δ 7.14–7.03 (m, 2H), 6.96 (dd, J = 10.2, 1.5 Hz, 1H), 6.87–6.79 (m, 1H), 6.81–6.71 (m, 3H), 6.55 (d, J = 7.7 Hz, 1H), 5.73 (dd, J = 10.2, 1.6 Hz, 1H), 3.64–3.59 (m, 3H), 2.65 (d, J = 1.6 Hz, 3H), 1.21–1.16 (m, 3H), 1.10 (s, 1H), 1.07 (s, 3H). ¹³C NMR (101 MHz, DMSO) δ 154.44, 148.32, 136.78, 130.24, 129.80, 127.91, 127.39, 121.92, 120.67, 119.70, 119.39, 119.11, 114.81, 107.24, 104.31, 51.83, 29.03, 26.14, 20.37. HRMS (ESI+), m/z [M + H]⁺: calculated: 278.1545; found: 278.1556. LCMS (CI+), m/z [M + H]⁺ = 278.2.

N,N-diethyl-1',3',3'-trimethyl-1',3'-dihydrospiro[chromene-2,2'-indol]-7-amine (**1 b**): ¹H NMR (400 MHz, DMSO- d_6) δ 7.12 (dd, J = 20.9, 5.5 Hz, 1H), 7.06 (t, J = 6.5 Hz, 2H), 6.90 (dd, J = 8.4, 3.1 Hz, 1H), 6.83 (dd, J = 10.2, 3.2 Hz, 1H), 6.74 (td, J = 7.4, 3.2 Hz, 1H), 6.53 (dd, J = 7.8, 3.2 Hz, 1H), 6.12 (dd, J = 8.6, 2.7 Hz, 1H), 5.88 (t, J = 2.8 Hz, 1H), 5.38 (dd, J = 10.2, 3.1 Hz, 1H), 3.57 (d, J = 3.1 Hz, 9H), 3.39 (dd, J = 8.4, 5.9 Hz, 1H), 3.23 (q, J = 6.6 Hz, 5H), 2.64 (d, J = 3.0 Hz, 3H), 1.62–1.51 (m, 1H), 1.46 (s, 1H), 1.30–1.19 (m, 4H), 1.11 (q, J = 5.7 Hz, 1H), 1.06 (d, J = 3.2 Hz, 3H), 1.01 (dd, J = 8.5, 5.4 Hz, 7H). ¹³C NMR (101 MHz, DMSO- d_6) δ 156.11, 149.50, 148.61, 137.15, 129.75, 128.11, 127.76, 121.89, 119.08, 113.45, 107.63, 107.12, 104.97, 104.57, 104.11, 96.99, 66.85, 51.45, 44.61, 44.12, 29.02, 26.33, 20.32, 12.96, 12.91. HRMS (ESI+), m/z [M + H]⁺: calculated: 349.2280; found: 349.2291. LCMS (CI+), m/z [M + H]⁺ = 349.2.

6-methoxy-1',3',3'-trimethyl-1',3'-dihydrospiro[chromene-2,2'-indole] (**1 c**): ¹H NMR (400 MHz, CdCl₂) δ 7.21–7.11 (m, 1H), 7.06 (dt, J = 7.2, 1.8 Hz, 1H), 6.87–6.76 (m, 2H), 6.70–6.59 (m, 2H), 6.59 (d, J = 2.7 Hz, 1H), 6.51 (dd, J = 7.7, 2.6 Hz, 1H), 5.69 (dd, J = 10.2, 2.4 Hz, 1H), 3.74 (d, J = 2.2 Hz, 3H), 2.71 (d, J = 2.4 Hz, 3H), 1.32–1.21 (m, 3H), 1.15 (d, J = 2.3 Hz, 3H). ¹³C NMR (101 MHz, DMSO- d_6) δ 153.34, 148.39, 136.86, 129.81, 127.88, 121.88, 120.49, 119.45, 119.29, 115.84, 115.39, 111.96, 107.18, 103.93, 66.85, 55.87, 51.72, 29.06, 26.16, 20.43. HRMS (ESI+), m/z [M + H]⁺: calculated: 308.1651; found: 308.1660. LCMS (CI+), m/z [M + H]⁺ = 308.2.

8-methoxy-1',3',3'-trimethyl-1',3'-dihydrospiro[chromene-2,2'-indole] (**1 d**): ¹H NMR (400 MHz, DMSO- d_6) δ 7.14–7.03 (m, 4H), 6.96 (d, J = 10.1 Hz, 2H), 6.83 (q, J = 4.2 Hz, 2H), 6.81–6.71 (m, 6H), 6.55 (d, J = 7.7 Hz, 2H), 5.73 (d, J = 10.1 Hz, 2H), 3.62 (s, 5H), 2.65 (s, 5H), 1.23 (s, 1H), 1.19 (s, 5H), 1.07 (s, 5H). HRMS (ESI+), m/z [M + H]⁺: calculated: 308.1651; found: 308.1653.

1',3',3'-trimethyl-1',3'-dihydrospiro[1,3-dioxolo[4,5-g]chromene-6,2'-indole] (**1 e**): ¹H NMR (400 MHz, DMSO- d_6) δ 7.12–6.99 (m, 4H), 6.88 (dd, J = 10.1, 3.4 Hz, 2H), 6.75 (q, J = 5.4 Hz, 4H), 6.53 (d, J = 7.7 Hz, 2H), 6.37 (d, J = 3.9 Hz, 1H), 5.91 (d, J = 3.4 Hz, 4H), 5.58 (dd, J = 10.1, 3.6 Hz, 2H), 2.76 (d, J = 9.0 Hz, 1H), 2.63 (d, J = 3.4 Hz, 5H), 1.56 (d, J = 13.8 Hz, 1H), 1.50–1.45 (m, 2H), 1.22 (d, J = 3.2 Hz, 5H), 1.06 (s, 5H). ¹³C NMR (101 MHz, DMSO- d_6) δ 150.08, 148.40, 148.24, 141.13, 136.85, 129.69, 127.86, 121.89, 119.29, 116.43, 111.69, 107.16, 106.37, 104.53, 101.40, 97.43, 51.52, 28.96, 26.18, 20.39. HRMS (ESI+), m/z [M + H]⁺: calculated: 322.1443; found: 322.1451. LCMS (CI+), m/z [M + H]⁺ = 322.2.

1',3',3'-trimethyl-6-phenyl-1',3'-dihydrospiro[chromene-2,2'-indole] (**1 f**): ¹H NMR (500 MHz, DMSO- d_6) δ 7.62–7.57 (m, 4H), 7.51 (q, J = 2.0 Hz, 2H), 7.45–7.35 (m, 6H), 7.33–7.26 (m, 2H), 7.11 (ddd, J = 10.6, 7.1, 2.3 Hz, 6H), 6.77 (ddd, J = 14.0, 7.8, 2.5 Hz, 4H), 6.57

(dd, $J=7.8, 2.4$ Hz, 2H), 5.82 (dd, $J=10.4, 2.5$ Hz, 2H), 2.70–2.65 (m, 6H), 2.63 (s, 1H), 1.46 (s, 1H), 1.39 (s, 1H), 1.24 (d, $J=2.4$ Hz, 6H), 1.11 (d, $J=2.2$ Hz, 6H). ^{13}C NMR (126 MHz, DMSO- d_6) δ 154.10, 148.30, 140.15, 136.74, 132.77, 129.88, 129.30, 128.46, 127.93, 127.21, 126.56, 125.63, 121.93, 120.14, 119.43, 119.40, 115.27, 107.27, 104.64, 51.89, 29.04, 26.17, 20.35. HRMS (ESI+), m/z , $[\text{M} + \text{H}]^+$: calculated: 354.1858; found: 354.1862. LCMS (CI+), m/z , $[\text{M} + \text{H}]^+ = 354.2$.

6-bromo-1',3',3'-trimethyl-1',3'-dihydrospiro[chromene-2,2'-indole] (1g): ^1H NMR (400 MHz, DMSO- d_6) δ 7.40 (d, $J=2.6$ Hz, 1H), 7.21 (dd, $J=8.6, 2.6$ Hz, 1H), 7.09 (td, $J=7.5, 5.3$ Hz, 2H), 7.00 (d, $J=10.3$ Hz, 1H), 6.76 (t, $J=7.4$ Hz, 1H), 6.63 (d, $J=8.7$ Hz, 1H), 6.55 (d, $J=7.6$ Hz, 1H), 5.83 (d, $J=10.3$ Hz, 1H), 2.66 (s, 1H), 2.63 (s, 3H), 1.28–1.04 (m, 7H). ^{13}C NMR (101 MHz, DMSO- d_6) δ 153.66, 148.15, 136.58, 132.50, 129.58, 128.77, 127.98, 121.93, 121.36, 121.15, 119.56, 117.13, 111.71, 107.31, 104.78, 52.01, 29.00, 26.12, 20.29. HRMS (ESI+), m/z , $[\text{M} + \text{H}]^+$: calculated: 356.0650; found: 356.0651. LCMS (CI+), m/z , $[\text{M} + \text{H}]^+ = 356.1$.

6-chloro-1',3',3'-trimethylspiro[chromene-2,2'-indole] (1h): ^1H NMR (400 MHz, CDCl_3) δ 7.18 (tdd, $J=7.6, 3.8, 2.1$ Hz, 1H), 7.11–7.05 (m, 1H), 7.03 (dq, $J=4.6, 2.7$ Hz, 2H), 6.86 (ddt, $J=10.9, 7.4, 3.4$ Hz, 1H), 6.79 (dd, $J=10.2, 3.5$ Hz, 1H), 6.64 (dd, $J=9.3, 3.5$ Hz, 1H), 6.53 (dd, $J=7.7, 3.5$ Hz, 1H), 5.74 (dd, $J=10.2, 3.4$ Hz, 1H), 2.72 (d, $J=3.4$ Hz, 3H), 2.05 (d, $J=3.4$ Hz, 3H), 1.34–1.23 (m, 4H), 1.17 (d, $J=3.4$ Hz, 3H). ^{13}C NMR (101 MHz, DMSO- d_6) δ 153.20, 148.16, 136.59, 129.63, 128.85, 127.98, 126.72, 124.12, 121.94, 121.23, 120.79, 119.54, 116.64, 107.30, 104.77, 52.01, 29.01, 26.13, 20.30. HRMS (ESI+), m/z , $[\text{M} + \text{H}]^+$: calculated: 312.1155; found: 312.1159. LCMS (CI+), m/z , $[\text{M} + \text{H}]^+ = 312.1$.

6,8-dichloro-1',3',3'-trimethyl-1',3'-dihydrospiro[chromene-2,2'-indole] (1i): ^1H NMR (400 MHz, DMSO- d_6) δ 7.57 (t, $J=2.2$ Hz, 1H), 7.46 (t, $J=2.1$ Hz, 1H), 7.20–7.06 (m, 2H), 7.02 (dd, $J=10.3, 1.7$ Hz, 1H), 6.78 (t, $J=7.4$ Hz, 1H), 6.62–6.56 (m, 1H), 5.90 (dd, $J=10.1, 1.7$ Hz, 1H), 2.63 (d, $J=1.7$ Hz, 3H), 1.53 (d, $J=14.4$ Hz, 3H), 1.28–1.18 (m, 4H), 1.11–1.06 (m, 3H). ^{13}C NMR (101 MHz, DMSO- d_6) δ 150.08, 147.87, 136.39, 134.45, 129.12, 128.47, 128.01, 122.44, 122.29, 121.89, 119.74, 111.87, 109.66, 107.36, 106.21, 66.85, 52.14, 28.96, 26.07, 20.34. HRMS (ESI+), m/z , $[\text{M} + \text{H}]^+$: calculated: 433.9750; found: 433.9752. LCMS (CI+), m/z , $[\text{M} + \text{H}]^+ = 434.2$.

6,8-dibromo-1',3',3'-trimethyl-1',3'-dihydrospiro[chromene-2,2'-indole] (1j): ^1H NMR (500 MHz, DMSO- d_6) δ 7.37 (t, $J=3.1$ Hz, 1H), 7.32 (t, $J=3.1$ Hz, 1H), 7.21–7.01 (m, 4H), 6.82–6.75 (m, 1H), 6.60 (dd, $J=7.8, 3.8$ Hz, 1H), 5.94 (dd, $J=10.2, 3.9$ Hz, 1H), 2.66 (d, $J=3.9$ Hz, 4H), 1.54 (dd, $J=14.7, 3.8$ Hz, 1H), 1.48–1.37 (m, 1H), 1.28–1.22 (m, 1H), 1.21 (d, $J=3.9$ Hz, 3H), 1.09 (d, $J=3.8$ Hz, 3H). HRMS (ESI+), m/z , $[\text{M} + \text{H}]^+$: calculated: 346.0765; found: 346.0770.

3-(3',3'-dimethylspiro[chromene-2,2'-indol]-1'(3'H)-yl)-*N,N,N*-trimethylpropan-1-aminium bromide (2a): ^1H NMR (300 MHz, CDCl_3) δ 7.17 (t, $J=7.6$ Hz, 1H), 7.12–7.02 (m, 3H), 6.93–6.78 (m, 3H), 6.62 (d, $J=8.5$ Hz, 1H), 6.54 (d, $J=7.7$ Hz, 1H), 5.66 (d, $J=10.2$ Hz, 1H), 3.56–3.18 (m, 4H), 3.11 (s, 9H), 2.27–1.78 (m, 5H), 1.30 (s, 3H), 1.13 (s, 3H). ^{13}C NMR (101 MHz, CDCl_3) δ 161.22, 160.89, 153.52, 146.20, 136.54, 129.98, 129.93, 127.83, 127.29, 122.02, 120.63, 119.54, 118.94, 114.74, 106.21, 118.55, 104.23, 64.99, 53.07, 52.12, 39.71, 25.99, 22.55, 20.15. LCMS (CI+), m/z , $[\text{M} + \text{H}]^+ = 363.0$.

3-(5'-methoxy-3',3'-dimethylspiro[chromene-2,2'-indol]-1'(3'H)-yl)-*N,N,N*-trimethylpropan-1-aminium bromide (2b): ^1H NMR (300 MHz, CDCl_3) δ 7.12–7.02 (m, 2H), 6.87 (d, $J=10.2$ Hz, 1H), 6.82 (td, $J=7.4, 1.2$ Hz, 1H), 6.74–6.66 (m, 2H), 6.63 (d, $J=7.6$ Hz, 1H), 6.46 (d, $J=8.1$ Hz, 1H), 5.65 (d, $J=10.2$ Hz, 1H), 3.77 (s, 3H), 3.57–3.21 (m, 4H), 3.17 (s, 9H), 2.25–1.77 (m, 5H), 1.27 (s, 3H), 1.14 (s, 3H). ^{13}C NMR (101 MHz, CDCl_3) δ 153.99, 153.62, 140.41, 138.23, 129.92, 127.24, 120.55, 118.99, 118.54, 114.77, 111.25, 110.12, 106.36,

104.67, 77.32, 77.00, 76.68, 65.09, 55.88, 53.12, 52.27, 40.13, 29.67, 25.89, 22.52, 20.09. LCMS (CI+), m/z , $[\text{M} + \text{H}]^+ = 393.0$.

1'-(3'-((1-oxidaneyl)dioxo-l6-sulfaneyl)propyl)-5'-methoxy-3',3'-dimethylspiro[chromene-2,2'-indoline] (2c): ^1H NMR (300 MHz, methanol- d_4) δ 8.69 (d, $J=16.4$ Hz, 1H), 8.10 (dd, $J=8.0, 1.4$ Hz, 1H), 7.83 (d, $J=9.1$ Hz, 1H), 7.78 (d, $J=17.1$ Hz, 1H), 7.43 (td, $J=7.8, 1.6$ Hz, 1H), 7.34 (d, $J=2.4$ Hz, 1H), 7.16 (dd, $J=8.9, 2.5$ Hz, 1H), 7.01 (t, $J=7.6, 1\text{H}$), 6.96 (dd, $J=8.3, 0.8$ Hz, 1H), 4.79 (m, 2H), 3.93 (s, 3H), 3.03 (t, $J=6.5$ Hz, 2H), 2.39 (m, 2H), 1.84 (s, 6H). LCMS (CI+), m/z , $[\text{M} + \text{H}]^+ = 416.0$.

Synthesis of N-Fmoc-3: The synthesis was performed following Scheme 1. Compounds **5** and **6** were obtained according to^[37]. To obtain Boc-3 (*N*-(tert-butoxycarbonyl)-3-[(*E*)-2-(5-methoxy-1,3,3-trimethyl-3*H*-indolium-2-yl)vinyl]-*L*-tyrosinate), compounds **5** (1 mmol) and **6** (1 mmol) were refluxed in CH_3CN (20 mL) in the presence of diisopropylethylamine (3 mmol) overnight. The mixture was diluted with equal amount of water and applied directly on a C18 FLC column. Boc-3 was eluted with a mixture of water/0.1% TFA/ CH_3CN . The colored fraction was collected and evaporated to obtain a red solid. To obtain Fmoc-3 (*N*-[(9*H*-fluoren-9-ylmethoxy)carbonyl]-3-[(*E*)-2-(5-methoxy-1,3,3-trimethyl-3*H*-indolium-2-yl)vinyl]-*L*-tyrosinate), first Boc-3 (1 mmol) was dissolved in a TFA/ CH_2Cl_2 mixture (50/50 v/v, 10 mL) and stirred at room temperature for 3 h. The solvents were removed in vacuum; the residue was dissolved in CH_3CN (10 mL), the obtained solution was combined with 5% aqueous solution of NaHCO_3 (10 mL) and Fmoc-OSu (1.1 mmol) was added. The resulting mixture was stirred at room temperature for 3 h. It was then diluted with water and purified on a C18 FLC column (water 0.1% TFA/ CH_3CN as an eluent). The colored fraction was collected and evaporated to obtain a red solid.

^1H NMR (300 MHz, methanol- d_4) δ 8.49 (d, $J=16.4$ Hz, 1H), 7.85 (d, $J=2.1$ Hz, 1H), 7.75 (d, $J=7.5$ Hz, 2H), 7.67 (d, $J=8.9$ Hz, 1H), 7.60–7.50 (m, 3H), 7.42–7.20 (m, 6H), 7.17 (dd, $J=8.9, 2.4$ Hz, 1H), 6.94 (d, $J=8.4$ Hz, 1H), 4.58 (dd, $J=10.3, 4.7$ Hz, 1H), 4.36 (dd, $J=9.0, 5.8$ Hz, 1H), 4.22–4.12 (m, 2H), 4.08 (d, $J=16.1$ Hz, 1H), 3.99 (s, 3H), 3.94 (s, 3H), 2.99 (dd, $J=14.1, 10.4$ Hz, 1H), 1.70 (d, $J=2.3$ Hz, 6H). LCMS (ESI+), m/z , $[\text{M} + \text{H}]^+ = 617.7$.

Peptide synthesis: The peptides were synthesized using a microwave-assisted Fmoc SPPS protocol on a CEM Liberty Blue peptide synthesizer. 2-Chlorotriylchloride resin was loaded with lysine residue using Fmoc-Lys(Boc)-OH (0.1 mmol, 1 equiv.). Next, a sequence of deprotection-coupling cycles was applied. Deprotection was performed at 50°C using $P_{\text{microwave}}=30$ W, for 210 s, applying piperidine (20 w% in DMF (dimethylformamide), 3 mL/deprotection step). The coupling was performed using the following conditions: $T=50^\circ\text{C}$, $P_{\text{microwave}}=30$ W, $t=600$ s an Fmoc-protected amino acid (0.2 M in DMF, 5 equiv., 2.5 mL/coupling step), DIC (diisopropylcarbodiimide, 0.5 M in DMF, 5 equiv., 1.0 mL/coupling step) and Oxyma (ethyl 2-cyano-2-(hydroxyimino)acetate, 1.0 M in DMF, 5 equiv., 0.5 mL/coupling) were used. After the last deprotection step, the resins were washed with DCM (dichloromethane, 3x), hexane (2x), and dried under vacuum. The peptides' final deprotection and cleavage were done manually with TFA (trifluoroacetate): H_2O :TIS (triisopropylsilane) (93:5:2, v/v/v; 10 mL); incubation for 1 h at r.t. The solutions were filtered, the solvent volume reduced by N_2 flow, followed by the (cold) diethyl ether precipitation. Precipitates were decanted, redissolved in 50% MeCN (0.1% TFA) and lyophilized to remove volatiles and purified by HPLC. All peptides were at least 95% pure (UV, 220 nm detection).

MALDI-MS, m/z : BP100, $[\text{M} + \text{H}]^+ = 1421$; BP100-7F, $[\text{M} + \text{H}]^+ = 1440$; BP100-7MC, $[\text{M} + \text{H}]^+ = 1684$; BP100-4,7MC, $[\text{M} + \text{H}]^+ = 1913$. Analytical HPLC (C18), 5–95% B, 15 min $^{-1}$; flow 1.5 mL/min; $R_t=8,1$ min

(BP100); = 8,1 min (BP100-7F); = 8,3 min (BP100-4MC); = 8,9 min (BP100-4,7MC);

Absorbance measurements were made in a quartz cuvette (Helma) with a pathlength of 10 mm, using Ultrospec 8000 (GE Healthcare) dual beam spectrophotometer. Model compounds were measured in methanol (MeOH) at ca. 10 μM concentration. The SP to the MC isomerization was studied in PBS at different pH values (10 mM PB, 100 mM NaCl, pH = 5, 6, 7, or 8, in each separate experiment). The peptide BP100-7MC was measured at 70,4 μM , BP100-4,7MC – 42.7 μM , and the spiropyran amino acid – 54.6 μM . The solutions were converted to SP photoform by visible light LED (Nichia, 450–700 nm; lighting current: 280 lm; 2 W/3 V) and the relaxation in the dark was monitored by time-dependent absorbance measurements. The half-life time of the relaxation in the dark was calculated from the first-order reaction kinetics, according to^[38].

Fluorescence measurements were performed using 10 mm path cuvette (Helma) at the concentration 16.7 μM for **3** and BP100-7MC; and at 8,35 μM for BP100-4,7MC. The spectra were recorded on a FluoroMax2 spectrofluorometer (HORIBA Jobin Yvon) equipped with a thermostated sample compartment. The excitation wavelength was set at 400 nm; 3 nm and 1 nm slits were typically used for excitation and emission channels, respectively. Data has been recorded with 1 nm intervals and 0,1 s integration time. Recordings in PB (10 mM) and in PB in the presence of excess SDS (5 mM) are shown in Supplementary Figure S5.

Sample preparation for CD. Peptides were dissolved in aqueous (PBS) buffers, 50% TFE or detergent solutions. PBS (10 mM, 140 mM NaF) was adjusted to pH 5.5 or 7.4 and used to obtain colloid solutions of SDS and DPC (final concentration 5 or 7 mM) and mixtures with TFE. For liposomes measurements, two protocols were applied: either the peptides were co-dissolved with the lipids in the organic solvents (see below) and prepared as proteobilayers, or the double-concentrated peptide suspensions in PB were gently mixed with the double-concentrated pre-formed LUVs. The latter preparations were co-incubated with the LUVs for 30 min at 35 °C to ensure binding. Both LUVs kinds were prepared by first co-dissolving the lipid (or lipid/peptide) mixtures in a 2:1 (v:v) mixture of chloroform:methanol. The solvent was removed under a N_2 stream, followed by an overnight vacuum exposure. The dry material was hydrated with preheated (35 °C) PBS and exposed to 10-time freeze (liq. N_2)- thaw (35 °C water bath) cycles. Finally, thawed suspensions were further homogenized in a high-power ultrasonic bath with a beaker-shaped sonotrode (UTR 200, Hielscher) and either directly measured (proteobilayers) or extruded (Avant mini extruder, 100 nm pores) according to manufacturer instructions.

CD measurements were performed on a J-815 instrument (Jasco) equipped with a home-built N_2 -flow regulator using a 1 mm path quartz cuvette (Helma). The measurements were performed at 25 °C, covering the 185–260 nm range. Per sample, 3 accumulations at 20 nm/min have been averaged. For the measurements of the SP photophorms, cuvette-loaded samples have been illuminated for at least 30 seconds (until full decoloration) by VIS light (400–700 nm) with a high-power light source (SUPERLITE 410, LUMATEC). Instantly after illumination, the cuvette was placed in the spectrometer, and the measurement was started. Per sample, 5 accumulations at 100 nm/min were realized.

Sample preparation for ssNMR. In each case, peptide-reconstituted and control membranes were prepared as static mechanically oriented (glass support) lipid multibilayers, as described previously.^[29,30] For preparing oriented DMPC-d54 and DMPG-d54, 2 mg of lipid was used; for the DOPE system, 6 mg were used. Dry lipid was co-dissolved in MeOH/ CHCl_3 , 1:2 v:v (1:9 v:v, DOPE) with

the peptides at 1:10 mol:mol peptide:lipid ratio (1:100, DOPE). The solutions were spread over 5 (10, DOPE) glass plates with the size: 7.5×15×0.1 mm (Paul Marienfeld, cover glass slides for microscopy), with less than 0.5 mg total material per slide. The slides were dried under vacuum overnight, stacked on top of each other and covered with an empty slide on top of the stack. The stacks were rehydrated for 16–24 h in a sealed plastic container in the saturated water atmosphere at 48 °C for DMPC-d54 and DMPG-d54, and at 4 °C for DOPE. Hydrated stacks were insulated by wrapping them with parafilm and a polyethylene foil. Samples containing DOPE were kept on ice before the NMR measurements. The samples for *in situ* photoswitching, after hydration, were insulated by placement in an one-edge-open glass container (inner dimensions: 7.7×2.2×15 mm, Paul Marienfeld) and the open edge sealed with parafilm.

SsNMR measurements were performed on a 500 MHz widebore spectrometer (Bruker, Avance III HD). The spectra were recorded using a Bruker static triple-resonance (HX(Y)) probe, possessing a flat coil adjusted to the dimensions of the oriented samples. For ³¹P ssNMR (at 202.46 MHz) spectra acquisition, a Hahn-echo pulse sequence with 90° pulses of 4 μs and an echo delay of 30 μs , and a two-pulse phase-modulated ¹H-decoupling (Bruker TPPM-20 decoupling sequence, 30 kHz). About 512 scans, separated by a recycle delay of 4 s, were accumulated. For ²H ssNMR (at 76.7 MHz) spectra acquisition, a solid-echo pulse sequence was used, with the 90° pulses of 5–6 μs and an interpulse delay of 24 μs . About 2000–10,000 scans, separated by a recycle delay of 0.5 s, were accumulated. The processing was performed by using standard Bruker TopSpin software.

Standard temperature regulating equipment of the Bruker spectrometer was used, automatically controlling the sample temperature by heating an externally cooled dry airflow (1600 L/h). At least 600 s pre-acquisition delay for the temperature equilibration was used when collecting the spectra at defined temperatures.

For *in situ* photoswitching, a white-light high-power LED (450–700 nm, Nichia; lighting current: 280 lm; 2 W/3 V) has been mounted in the vicinity of the sample (< 1.5 cm, see Figure 6B) and continuous illumination applied during entire measurement.

Plant cell culture. The transgenic actin marker strain GF-11^[39] of tobacco BY-2 (*Nicotiana tabacum* L. cv “Bright Yellow 2”) has been used in cytotoxicity evaluation and for actin dynamics analysis. The strain stably expresses a green fluorescent protein (GFP) fusion with the *Arabidopsis thaliana* fimbrin actin-binding domain 2 (GFP-AtFABD2) and allows visualization of the actin fibres by observing the GFP fluorescence. The cells have been cultivated in a liquid medium containing 4.3 g/L Murashige and Skoog basal salt mixture, 30 g/L sucrose, 200 mg/L KH_2PO_4 , 100 mg/L inositol, 1 mg/L thiamine, and 0.2 mg/L (0.9 μM) 2,4-dichlorophenoxyacetic acid, at pH of 5.8. The cells were subcultured weekly by inoculating of 1.5 mL of stationary cells into fresh medium (30 mL) in a 100 mL Erlenmeyer flask. Inoculates were supplemented with 30 mg/L hygromycin to maintain selective stringency. The cultures were maintained in the dark at 26 °C under constant shaking on an IKA KS260 basic orbital shaker at 150 rpm.

Plant cell cytotoxicity evaluation. For cytotoxicity evaluation, the cells were used during their exponential growth phase (3-day post subculture) in the 6-well culture plates (2 mL per well). After adding the control and MC-photoform BP100 peptides, the cells were incubated for 24 h in the dark at 26 °C while shaking. The peptides were added from the medium stocks (ca. 1 mg/mL) without the volume adjustment. The Evans Blue exclusion test^[40] was used to quantify cell mortality. Aliquots of cell suspension (0.5 mL) were transferred into custom-made chambers to remove the medium, and the cells were incubated in 2.5% (w/v) Evans Blue (Merck) for

5 min. Unbound dye and the peptides were removed by washing (5×) with the fresh medium. The suspensions were diluted 1:3 with water, and 40 μL aliquots (per slide) were used for microscopy. The frequency of the dead cells was scored under a light microscope (Zeiss-Axioskop 2 FS, DIC illumination, ×10 objective). The values reported are based on the observation of 1000–1500 cells.

During the *in situ* cytotoxicity photoswitching experiments, the cells were incubated with the peptides in small Petri dishes with a diameter of 30 mm. Before the addition of the peptide to the cells, BP100-7MC and BP100-4,7MC were converted into SP-photoform with a white light LED (450–700 nm, Nichia; lighting current: 280 lm; 2 W/3 V) until visible decoloration. After the peptides have been added to the cell culture and the Petri dish was put on a shaker, the LED was mounted on top of the dish with a duct tape. Incubation time under continuous illumination was reduced to 2 h.

Evaluation of actin filament dynamics. For the time-dependent microscopy, GF-11 cells were used during their stationary growth phase (7-day post subculture). First, 50 μL of the cell suspension was diluted to 1 mL, and peptides were mixed at 5 μM final concentration. Immediately, 40 μL of the suspension was added to a microscope slide, exposed for 5 min to white light LED illumination (450–700 nm, Nichia; lighting current: 280 lm; 2 W/3 V) and analysed (at the darkness) by confocal time-lapse microscopy. Confocal images were recorded with an AxioObserver Z1 (Carl Zeiss), equipped with a CCD camera (AxioCam MRm), using a 63× LCI-NeofluarImmCorr DIC objective (NA 1.3). Under excitation at 488 nm (GFP), 5 Z-stack images through the cells' cortical region at an arbitrarily selected cell were collected and observed for 180 s at 30 s intervals. Collected Z-stack image averages were used for the analysis as was described previously.^[33,34]

Antibacterial activity measurements. *Escherichia coli* strain DSM 1103 (=ATCC 25922) obtained from the German collection of microorganisms and cell cultures (DSMZ, Braunschweig, Germany) has been used.

Test cultures, inoculated with cells grown overnight, were obtained in standard Mueller-Hinton (MH) broth (Carl Roth) medium by cultivation up to mid-exponential growth phase ($OD_{550} \sim 4.0$), using 100 mL Erlenmeyer culture flasks (20 mL culture volume) and cultivating at 37 °C under agitation (Heidolph Unimax Unimax 1010, equipped with a heating module).

The cultures were diluted until ($OD_{500} \sim 0.1$) with pre-warmed MH broth media, where pH was adjusted to either 5, 6 or 7 (by HCl addition). The dilutions were placed into disposable spectrophotometer cuvettes (2 mL) and the peptides (from aqueous stocks) were added in not more than 50–100 μL volumes. Peptide activities were monitored by direct measuring of OD_{500} taken at 0, 20, 40, 80, 120 min and overnight. When not measured, the cuvettes were incubated under agitation at 37 °C. The “dark”-designated samples (MC/MCH⁺ photoform enriched) were wrapped in an aluminum foil; the “light”-designated ones (SP photophorm enriched) were kept under illumination of the white-light mercury lamps. (Irradiance and emission spectra were not determined).

Acknowledgements

The authors acknowledge EU funding by EU H2020-MSCA-RISE through the PELICO (grant 690973) and ALISE (grant 101007256) projects. This work was also supported by DFG-GRK 2039 (A. H., S. A., A. S. U.) and BMBF-VIP+ (O. B., A. S. U.). Authors are thankful to academician of NAS of Ukraine, professor O. Ishchenko for useful discussion regarding merocya-

nine properties and to all defenders of Ukraine who allow to continue scientific work for Ukrainian citizens and, hence, contribute to completion of this research. Open Access funding enabled and organized by Projekt DEAL.

Conflict of Interests

The authors declare no conflict of interest.

Data Availability Statement

The data that support the findings of this study are available in the supplementary material of this article.

Keywords: BP100 · membrane-active peptides · molecular photoswitches · photopharmacology · spiropyran

- [1] M. Muttenthaler, G. F. King, D. J. Adams, P. F. Alewood, *Nat. Rev. Drug Discovery* **2021**, *20*, 309.
- [2] a) M. Goodman, A. Kossoy, *J. Am. Chem. Soc.* **1966**, *88*, 5010; b) M. Goodman, M. L. Falxa, *J. Am. Chem. Soc.* **1967**, *89*, 3863.
- [3] a) O. Pieroni, A. Fissi, G. Popova, *Progr. Polym. Sci.* **1998**, *23*, 81; b) O. Pieroni, A. Fissi, N. Angelini, F. Lenci, *Acc. Chem. Res.* **2001**, *34*, 9; c) C. Renner, L. Moroder, *ChemBioChem* **2006**, *7*, 868; d) J. E. Bock, J. Gavenonis, J. A. Kritzer, *ACS Chem. Biol.* **2013**, *8*, 488; e) R. J. Mart, R. J. Errington, C. L. Watkins, S. C. Chappell, M. Wiltshire, A. T. Jones, P. J. Smith, R. K. Allemann, *Mol. BioSyst.* **2013**, *9*, 2597; f) S. Wiedbrauk, H. Dube, *Tetrahedron Lett.* **2015**, *56*, 4266; g) R. J. Mart, R. K. Allemann, *Chem. Commun.* **2016**, *52*, 12262; h) S. Kitzig, M. Thilemann, T. Cordes, K. Rück-Braun, *ChemPhysChem* **2016**, *17*, 1252; i) L. Albert, O. Vázquez, *Chem. Commun.* **2019**, *55*, 10192; j) T. C. de Souza-Guerreiro, G. Bondelli, I. Grobas, S. Donini, V. Sesti, C. Bertarelli, G. Lanzani, M. Asally, G. M. Paternò, *Adv. Sci.* **2023**, *10*, 2205007; k) F. Höglsparger, B. E. Vos, A. D. Hofemeier, M. D. Seyfried, B. Stövesand, A. Alavizargar, L. Topp, A. Heuer, T. Betz, B. J. Ravoo, *Nat. Commun.* **2023**, *14*, 3760.
- [4] a) W. A. Velema, W. Szymanski, B. L. Feringa, *J. Am. Chem. Soc.* **2014**, *136*, 2178; b) J. Broichhagen, J. A. Frank, D. Trauner, *Acc. Chem. Res.* **2015**, *48*, 1947; c) M. M. Lerch, M. J. Hansen, G. M. van Dam, W. Szymanski, B. L. Feringa, *Angew. Chem. Int. Ed.* **2016**, *55*, 10978; d) K. Hüll, J. Morstein, D. Trauner, *Chem. Rev.* **2018**, *118*, 10710.
- [5] a) E. Fischer, Y. Hirshberg, *J. Chem. Soc.* **1952**, 4522; b) Y. Hirshberg, E. Fischer, *J. Chem. Soc.* **1953**, 629; c) G. Berkovic, V. Krongauz, V. Weiss, *Chem. Rev.* **2000**, *100*, 1741; d) V. I. Minkin, *Chem. Rev.* **2004**, *104*, 2751; e) R. Klajn, *Chem. Soc. Rev.* **2014**, *43*, 148; f) L. Kortekaas, W. R. Browne, *Chem. Soc. Rev.* **2019**, *48*, 3406.
- [6] a) J. Andersson, S. Li, P. Lincoln, J. Andréasson, *J. Am. Chem. Soc.* **2008**, *130*, 11836; b) W. A. Velema, M. J. Hansen, M. M. Lerch, A. J. Driessen, W. Szymanski, B. L. Feringa, *Bioconjugate Chem.* **2015**, *26*, 2592.
- [7] a) E. Zahavy, S. Rubin, I. Willner, *Mol. Cryst. Liq. Cryst. Sci. Technol. Sect. A* **1994**, *246*, 195; b) A. Fissi, O. Pieroni, N. Angelini, F. Lenci, *Macromolecules* **1999**, *32*, 7116; c) T. M. Cooper, L. V. Natarajan, C. G. Miller, *Photochem. Photobiol.* **1999**, *69*, 173; d) K. Fujimoto, M. Amano, Y. Horibe, M. Inouye, *Org. Lett.* **2006**, *8*, 285.
- [8] a) K. Y. Tomizaki, H. Mihara, *J. Mater. Chem.* **2005**, *15*, 2732; b) K. Y. Tomizaki, H. Mihara, *Mol. BioSyst.* **2006**, *2*, 580.
- [9] L. Chen, J. Wu, C. Schmuck, H. Tian, *Chem. Commun.* **2014**, *50*, 6443.
- [10] a) Z. Qiu, H. Yu, J. Li, Y. Wang, Y. Zhang, *Chem. Commun.* **2009**, 3342; b) W. Wang, J. Hu, M. Zheng, L. Zheng, H. Wang, Y. Zhang, *Org. Biomol. Chem.* **2015**, *13*, 11492.
- [11] L. Chen, Y. Zhu, D. Yang, R. Zou, J. Wu, H. Tian, *Sci. Rep.* **2014**, *4*, 1.
- [12] The paper of Tomizaki, et al.^[8a] described the use of lysine-derived spiropyran derivatives in peptide synthesis. However, this work was not focused on the amino acid design and synthesis.
- [13] Y. Huan, Q. Kong, H. Mo, H. Yi, *Front. Microbiol.* **2020**, *11*, 2559.
- [14] B. Apellániz, N. Huarte, E. Largo, J. L. Nieva, *Chem. Phys. Lipids* **2014**, *181*, 40.

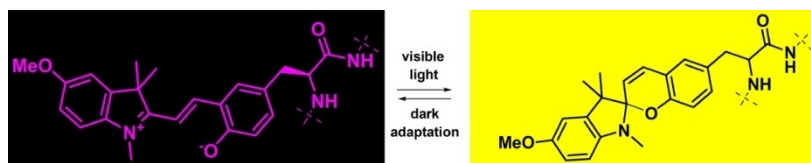
- [15] K. Desale, K. Kuche, S. Jain, *Biomater. Sci.* **2021**, *9*, 1153.
- [16] F. G. Avci, A. B. Sariyar, E. Ozkirimli, *Biomol. Eng.* **2018**, *8*, 77.
- [17] a) I. Shimizu, H. Kokado, E. Inoue, *Bull. Chem. Soc. Jpn.* **1969**, *42*, 1730; b) J. Zhou, Y. Li, Y. Tang, F. Zhao, X. Song, E. Li, *J. Photochem. Photobiol. A* **1995**, *90*, 117.
- [18] a) T. Stafforst, D. Hilvert, *Chem. Commun.* **2009**, 287; b) C. Özçoban, T. Halbritter, S. Steinwand, L. M. Herzig, J. Kohl-Landgraf, N. Askari, F. Groher, B. Fürtig, C. Richter, H. Schwalbe, B. Suess, J. Wachtveitl, A. Heckel, *Org. Lett.* **2015**, *17*, 1517.
- [19] K. Nepali, H. Y. Lee, J. P. Liou, *J. Med. Chem.* **2018**, *62*, 2851.
- [20] a) C. J. Roxburgh, P. G. Sammes, A. Abdullah, *Dyes Pigm.* **2009**, *83*, 31; b) E. I. Balmond, B. K. Tautges, A. L. Faulkner, V. W. Or, B. M. Hodur, J. T. Shaw, A. Y. Louie, *J. Org. Chem.* **2016**, *81*, 8744; c) M. Schulz-Senft, P. J. Gates, F. D. Sönnichsen, A. Staubitz, *Dyes Pigm.* **2017**, *136*, 292.
- [21] a) Z. Shi, P. Peng, D. Strohecker, Y. Liao, *J. Am. Chem. Soc.* **2011**, *133*, 14699; b) V. K. Johns, Z. Wang, X. Li, Y. Liao, *J. Phys. Chem. A* **2013**, *117*, 13101; c) C. Fu, J. Xu, C. Boyer, *Chem. Commun.* **2016**, *52*, 7126; d) H. Gao, T. Guo, Y. Chen, Y. Kong, Z. Peng, *J. Mol. Struct.* **2016**, *1123*, 426; e) D. Moldenhauer, F. Gröhn, *Chem. Eur. J.* **2017**, *23*, 3966.
- [22] L. Kortekaas, J. Chen, D. Jacquemin, W. R. Browne, *J. Phys. Chem. B* **2018**, *122*, 6423.
- [23] E. Badosa, R. Ferre, M. Planas, L. Feliu, E. Besalú, J. Cabrefiga, E. Bardají, E. Montesinos, *Peptides* **2007**, *28*, 2276.
- [24] P. Wadhwani, E. Strandberg, J. van den Berg, C. Mink, J. Bürck, R. A. M. Ciriello, A. S. Ulrich, *Biochim. Biophys. Acta* **2014**, *1838*, 940.
- [25] A. Roos, W. F. Boron, *Physiol. Rev.* **1981**, *61*, 296.
- [26] a) S. R. Keum, M. S. Hur, P. M. Kazmaier, E. Buncel, *Can. J. Chem.* **1991**, *69*, 1940; b) X. Song, J. Zhou, Y. Li, Y. Tang, *J. Photochem. Photobiol. A* **1995**, *92*, 99.
- [27] L. Cui, H. Zhang, G. Zhang, Y. Zhou, L. Fan, L. Shi, C. Zhang, S. Shuang, C. Dong, *Spectrochim. Acta Part A* **2018**, *202*, 13.
- [28] N. W. Tyer Jr, R. S. Becker, *J. Am. Chem. Soc.* **1970**, *92*, 1289.
- [29] a) S. L. Grage, S. Afonin, S. Kara, G. Buth, A. S. Ulrich, *Front. Cell Dev Biol.* **2016**, *4*, 65; b) J. Misiewicz, S. Afonin, A. S. Ulrich, *Biochim. Biophys. Acta* **2015**, *1848*, 833.
- [30] a) S. Pujals, H. Miyamae, S. Afonin, T. Murayama, H. Hirose, I. Nakase, K. Taniuchi, M. Umeda, K. Sakamoto, A. S. Ulrich, S. Futaki, *ACS Chem. Biol.* **2013**, *8*, 1894; b) W. Y. Hsu, T. Masuda, S. Afonin, T. Sakai, J. V. V. Arafiles, K. Kawano, H. Hirose, M. Imanishi, A. S. Ulrich, S. Futaki, *Bioorg. Med. Chem. Lett.* **2020**, *30*, 127190; c) M. Nishimura, Y. Kawaguchi, K. Kuroki, Y. Nakagawa, T. Masuda, T. Sakai, K. Kawano, H. Hirose, M. Imanishi, T. Takatani-Nakase, S. Afonin, A. S. Ulrich, S. Futaki, *Chem. Eur. J.* **2023**, *29*, e202300129.
- [31] T. Nagata, Y. Nemoto, S. Hasezawa, *Int. Rev. Cytol.* **1992**, *132*, 1.
- [32] I. M. Torcato, Y. H. Huang, H. G. Franquelim, D. Gaspar, D. J. Craik, M. A. Castanho, S. T. Henriques, *Biochim. Biophys. Acta Biomembr.* **2013**, *1828*, 944.
- [33] K. Eggenberger, P. Sanyal, S. Hundt, P. Wadhwani, A. S. Ulrich, P. Nick, *Plant Cell Physiol.* **2017**, *581*, 71.
- [34] H. Wang, M. Riemann, Q. Liu, J. Siegrist, P. Nick, *Plant Sci.* **2021**, *302*, 110712.
- [35] a) J. G. Pargaonkar, S. K. Patil, S. N. Vajekar, *Synth. Commun.* **2018**, *48*, 208; b) A. V. Chernyshev, M. S. Chernov'yants, E. N. Voloshina, N. A. Voloshin, *Russ. J. Gen. Chem.* **2002**, *72*, 1468; c) Q. Qi, J. Qian, S. Ma, B. Xu, S. X. A. Zhang, W. Tian, *Chem. Eur. J.* **2015**, *21*, 1149; d) A. V. Metelitsa, N. V. Stankevich, G. V. Shilov, B. S. Lukyanov, *Russ. J. Gen. Chem.* **2021**, *91*, 7; e) C. Balny, A. Hinnen, M. Mosse, *Tetrahedron Lett.* **1968**, *9*, 5097; f) S.-R. Keum, K.-B. Lee, P. M. Kazmaier, R. A. Manderville, E. Buncel, *Magn. Reson. Chem.* **1992**, *30*, 1128.
- [36] a) H. Hyun, E. A. Owens, H. Wada, A. Levitz, G. Park, M. H. Park, J. V. Frangioni, M. Henary, H. S. Choi, *Angew. Chem. Int. Ed.* **2015**, *54*, 8648; b) L. Wimberger, S. K. K. Prasad, M. D. Peeks, J. Andréasson, T. W. Schmidt, J. E. Beves, *J. Am. Chem. Soc.* **2021**, *143*, 20758.
- [37] a) M. E. Jung, T. I. Lazarova, *J. Org. Chem.* **1999**, *64*, 2976; b) S. L. Potisek, D. A. Davis, N. R. Sottos, S. R. White, J. S. Moore, *J. Am. Chem. Soc.* **2007**, *129*, 13808.
- [38] S. Kwangmettamat, T. Kudernac, *Chem. Commun.* **2018**, *54*, 5311.
- [39] T. Sano, T. Higaki, Y. Oda, T. Hayashi, S. Hasezawa, *Plant J.* **2005**, *44*, 595.
- [40] C. Morera, M. A. Villanueva, *World J. Microbiol. Biotechnol.* **2009**, *25*, 1125.

Manuscript received: January 8, 2024

Accepted manuscript online: February 17, 2024

Version of record online: ■■■■■

RESEARCH ARTICLE



A spiropyran-derived α -amino acid was carefully designed for the synthesis of photocontrollable bioactive peptides. Dramatic changes in structure and polarity occurring upon light exposure or dark adaptation of the spiropyran side chain can

cause changes in the behavior of peptides in lipid membranes and living cells, as demonstrated on spiropyran-containing analogs of the membrane-active peptide BP100 (KKLFKKILKYL-NH₂).

A. Hrebonkin, Dr. S. Afonin*, Dr. A. Nikitjuka, Dr. O. V. Borysov, Dr. G. Leitis, Dr. O. Babii, Dr. S. Koniev, T. Lorig, Dr. S. L. Grage, Prof. Dr. P. Nick, Prof. Dr. A. S. Ulrich*, Prof. Dr. A. Jirgensons, Prof. Dr. I. V. Komarov*

1 – 14

Spiropyran-Based Photoisomerizable α -Amino Acid for Membrane-Active Peptide Modification

